Supporting Information for:

High-Throughput Simulations Reveal Membrane-Mediated Effects of Alcohols on MscL Gating

Manuel N. Melo, Clément Arnarez, Hendrik Sikkema, Neeraj Kumar, Martin Walko, Herman J. C. Berendsen, Armagan Kocer, Siewert J. Marrink and Helgi I. Ingólfsson

Supplementary Methods

Detailed simulation set up

The initial systems were energy-minimized (steepest descent, 500 steps) and simulated for 1 ns using short time step 1-10 fs simulations with position restraints on the protein backbone. For all following simulations the restraints were released and the time step set to 30 fs. Coulomb interactions were screened by a relative permittivity constant $\varepsilon_r = 15$ and shifted to zero between 0 and 1.2 nm. Temperature was kept at 298 K using the Berendsen thermostat with a relaxation time constant $\tau_T = 1.0$ ps.[1] Each bilayer environment/condition was first simulated for 5 μs without applied membrane tension (MT). A semi-isotropic pressure-coupling scheme was used, with a compressibility of $3 \cdot 10^{-4}$ bar^{-1}, and pressure kept a 1 bar using the Berendsen barostat[1] with a relaxation time constant $\tau_p = 3.0$ ps, separately in the xy and z dimensions. For each condition MT was applied to select frames between 4-5 μs, see Table S1. MT was incrementally raised in a series of seven short (3 ns long) simulations, using a $\tau_p = 0.3$ ps and a compressibility of $3 \cdot 10^{-5}$ bar^{-1}. MT was fixed at 65 or 70 mN/m and multiple repeats simulated for 6 μs each, using a $\tau_p = 3.0$ ps. For selected simulations the same procedure was reversed to

remove the MT and those simulations were further extended by 6 μs, see Table S1. Higher applied tension will promote faster channel opening but will also increase the risk of bilayer rupturing. These processes are influenced by absolute applied tension and amplitude of the tension fluctuations, which to some extent can be controlled by adjusting τ_p and compressibility. In all the simulations alcohol concentrations were set as the average alcohol-to-lipid mol % in the bilayer; see Table S1 for lipid and alcohol counts in each simulation.

It is worth noting that all simulation times reported are actual simulated times and were not scaled to correct for the speedup present in CG models. Compared to AA models CG models have a reduced friction due to the reduced degrees of freedom, which can result in faster dynamics. The effective speedup is not the same for all systems but is often pegged at ~4-fold, corresponding to the speedup of CG water and lipids compared to their atomistic counterparts.[2]

Martini force fields

All simulations were performed using the Martini coarse-grain (CG) model v2.1.[2,3] The initial structure and topology of MscL was derived from the crystal structure of the closed state Tb-MscL (PDB ID 2OAR)[4,5] using *martinize* v1.0 (see www.cgmartini.nl) with no added elastic network. MscL is a homopentamer so a topology was derived for the monomer and replicated five times and secondary structure was predicted using the DSSP algorithm[6]. For the lipids, the original x5 bead (CCDCC) tail DOPC model[2] was used and for DEPC the tail was expanded by one C1 type bead (representing x4 CH_2) to a x6 bead (CCCDCC) tail. For the straight chain alcohols the models for 1-ethanol (eth) and 1-octanol (oct) are from the original Martini v2.0 model and 1-dodecanol (dodec) and 1-hexadecanol (hexdec) are based on 1-octanol with an extended tail (1-2 added C1 beads) in the same way as dodecane and hexadecane.[2] In the octanol exclusion (oct Excl) simulations the force field was modified in such a way that octanol interacts

normally with octanol, water and lipids while it is effectively excluded from interacting with MscL. This was done by changing the non-bonded interaction of octanol's P1 bead (renamed to eP1) with all the beads in MscL to Martini's weakest interaction level (level IX^2), while keeping all other interactions, including eP1 interactions with octanol, water and lipids beads, the same. All the used force fields can be found at the Martini portal www.cgmartini.nl.

MscL profile, pore area and constriction

In Figs. 1C and 5B contours are used to show the profile of MscL, obtained as follows: for each MscL bead a 5-element ring was defined, comprised of the five copies of said bead over the MscL homopentamer. The radius-of-gyration of each ring was then computed for each trajectory frame, together with the *z*-distance between the ring and bilayer centers-of-mass. An occupancy map was then summed on a 2D counting grid of cell size 0.01 nm, in which the horizontal dimension is the radius and the vertical is the *z*-distance to the bilayer center: for each frame and bead ring a circle of radius 0.47 nm was overlaid on the grid, centered at coordinates (radius, *z*-distance), increasing the occupancy of all underlying cells by 1 (0.47 nm was chosen as it is the Lennard-Jones size parameter σ of Martini beads). Profiles were drawn from the occupancy maps as iso-occupancy lines. For MscL the contour threshold was set as 10% of maximum occupancy. For clarity, the cytoplasmic helices of MscL (starting at residue 101) were excluded when calculating occupancies and contours.

MscL pore opening was monitored over time either as the pore area of select residues, or as the radius of the pore constriction residue ring. The pore area was estimated as the area of the pentagon formed by five monomer backbones at residues number 12, 15, 20, and 41, corresponding to different membrane depths (see Fig. S1A). The pore constriction refers to the tightest such ring of residues at any moment in time. For ease of comparison with the Martini

bead size the constriction is expressed as the constriction radius, and corresponds to the radius-of-gyration of said 5-element tightest-residue ring (Fig. S2), analogously to the radial size used for the profile calculation.

MscL water flux

Water flux was computed by analyzing water bead positions along trajectory frames. A channel crossing was counted when a water bead successively crossed two virtual gateways defined by the five backbone beads of either residue 36 (at the top of the channel pore), or residue 17 (at the bottom of the pore). A two-threshold approach was chosen because a single-threshold alternative was found to yield too much flickering noise due to water particles lingering at the threshold position. Care had to be taken in order to distinguish effective crossings through the channel, and not mere diffusion through the membrane or over periodic z images of the system. Proper diffusion path assignment requires a fairly high trajectory frame rate (90 ps/frame was used). The implementation of this flux counter is freely available online at www.cgmartini.nl.

MscL time to opening

After applied MT water flux across the MscL was monitored (see above). The first time when 3 CG waters (corresponding to 12 atomistic waters) traversed the channels gate in a window of 1.8 ns or less the channel was considered to open. Higher and lower thresholds were also tested and all gave very similar results (data not shown), except when setting the threshold at a single water bead flux—presumably due to occasional water slippage through still closed channels. For each bilayer environment/condition channel opening was measured for 30–100 simulations, started from 3–5 different starting structure equilibrated for 4–5 μs with no MT, see

Table S1. Most simulations—including all where MscL had not open yet—were extended to 6 μs, except in a handful of cases were the bilayer ruptured, see Tables S1 and S2. For each bilayer environment/condition the time to MscL channel opening was compared using Kaplan–Meier plots made with the survival model fit in Wolfram Research, Inc., Mathematica, Version 9; see Fig. S2. The open channel fraction was fit using a single exponential decay with a delay ($y = e^{-\lambda(x-d)}$) using the nonlinear model fit of the same software. The few simulations where the bilayer ruptured before the channel opened were excluded from this analysis. All data fits are shown in Fig S3 and the summary for each condition and fit output are listed in Table S2. The time when half the population of the channels is expected to be opened ($t_{½}$) was estimated from the best fit parameter for λ and d, $0.5 = e^{-\lambda(x-d)}$. The error was estimated from the propagated standard error of the best-fit parameter and also as the max/min of the parameters 95% confidence intervals (see Table S2).

Octanol occupancy/binding

In Fig. 5B octanol density and phosphate group (PO4 beads) contours were added to MscL profiles of the open channel. Both octanol and PO4 representations are based on occupancy maps obtained similarly to MscL's (see above). Their *z* position was defined as for MscL, as the *z*-distance to the bilayer center. The radial distance of octanol and PO4 was determined as the *xy*-distance to MscL's center-of-mass; it was calculated differently than for MscL because octanol and PO4 beads are isotropically disperse in the membrane plane, unconstrained to the homopentamer configuration of MscL. Occupancies were further corrected for radial distortion, by normalizing each radial position bin by the area it sweeps. For the PO4 contours a threshold was chosen at 50% of maximum normalized occupancy. In Fig. 5B octanol

occupancy is presented in a non-contour fashion, with color intensity normalized between white (zero occupancy) and the darkest blue (maximum occupancy).

To probe for specific octanol–MscL interactions the normalized contacts between the two are plotted for octanol in Fig. S7. A contact was defined as an octanol bead lying within 0.7 nm of a protein bead. The same octanol bead was allowed to be defined in-contact with more than one residue. For greater sensitivity at low contact counts, monomers were not discriminated, i.e., a contact with a given residue in one monomer counts as if all equivalent residues were also in contact. For reference, the normalized contacts for the lipids linker region (GL1 and GL2 beads) were also calculated in the same manner.

Bilayer properties analysis

To compare the different bilayer environments several bilayer properties were calculated from simulation with the same bilayers/added alcohols but without an MscL channel. Each bilayer condition was simulated for 4 μs; membrane tension (MT) was applied using the same protocol as descried above and further simulated with MT of 65 mN/m for 4 μs. The initial 1 μs and first 1 μs after applying MT were excluded from analysis; for the remaining trajectories the area per lipid, area compressibility, average tail order parameter, lipid diffusion, and bilayer thickness were analyzed both with and without MT. The area per lipid (A_l) was calculated from the average box area in the plane of the bilayer divided by the number of lipids in each leaflet. The bilayer area compressibility modulus (K_A) was calculated from the amplitude of the box area fluctuations:

$$K_\mathrm{A} = \frac{kT\langle \mathrm{A} \rangle}{N\langle (A-A_0)^2 \rangle},$$

where kT is the Boltzmann constant and temperature in Kelvin, N is the number of lipids in a leaflet/monolayer, A the box area, and A_0 the equilibrium area. The average tail order parameter

was calculated as the absolute average of all the lipid tail order parameter (*S*) of the bonds between the lipid tail beads and glycerol linker to tail beads. *S* was calculated from the angle θ between the normal of the bilayer surface and the vector along each bond, following:

$$S = \frac{1}{2}(3\langle(\cos\theta\,)^2\rangle - 1).$$

The lipid lateral diffusion was calculated from the mean square displacement (MSD) of the lipids phosphate (PO4) beads in the membrane plane.

$$MSD = \langle|r(t + t_0) - r(t_0)|^2\rangle,$$

where $|r(t + t_0) - r(t_0)|$ is the lateral distance travelled between times t and $t + t_0$ of the lipids PO4 beads. The center of mass motion of the system was removed and the MSD curve was fitted to $y = 4Dt + c$, to obtain *D*, the lateral diffusion constant using the g_msd tool in GROMACS[7], omitting 10% of the data at both ends. The bilayer thickness was measured as the distance between the centers of mass of the PO4 beads of the lipids in the two leaflets. All reported errors are standard errors of the mean obtained from block averaging, except for lipid diffusion where the error is the fit error as reported by the g_msd tool.

The lateral pressure profile (LPP) for each bilayer environment/condition was determined following the same formalism as described previously[8,9] using a modified version of the GROMACS package, available via www.gromacs.org. Briefly, the lateral pressure was obtained as the difference between the lateral, P_L, and normal, P_N, components of pressure tensor; $P_L=(P_{XX}+P_{YY})/2$ and $P_N=P_{ZZ}$. In practice the system is divided into a 3D grid with a 0.15 nm cell size. The local pressure tensor is analyzed for each grid point, averages are calculated for the xy plane along the z-axis (the normal of the bilayer), and a cubic spline applied to smooth the final graph. For all LPP calculations separate simulations were run using the same set up as above, but with smaller bilayer patches (280-286 lipids per bilayer depending on alcohol concentration), each simulated for 6 μs; see Table S1.

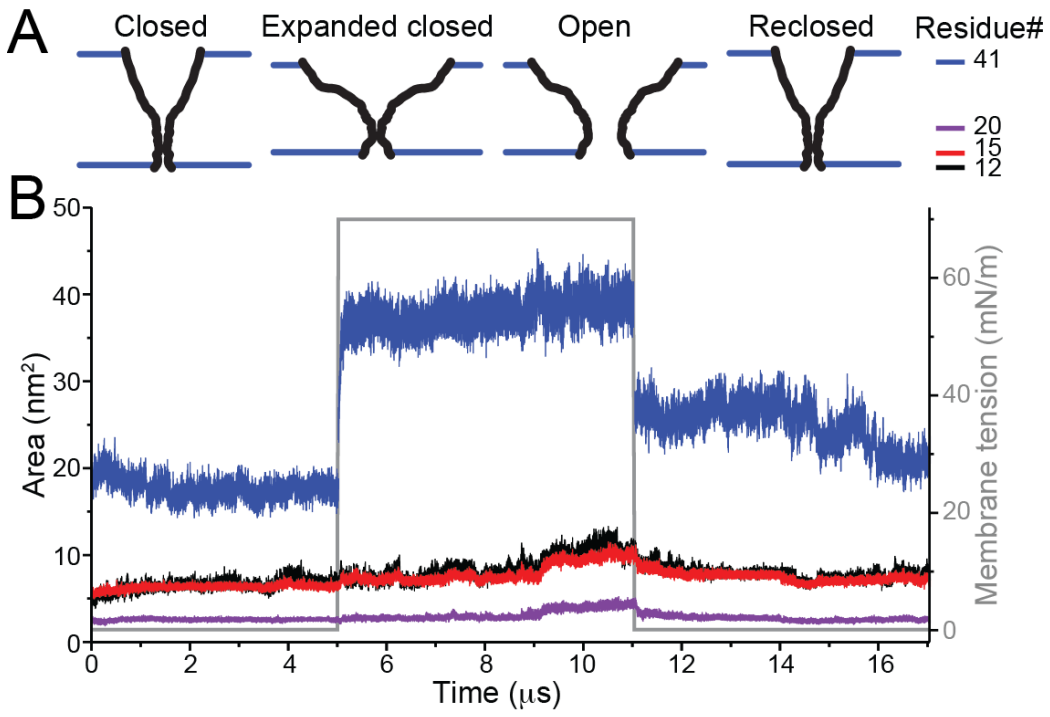

Figure S1. MscL gating. A) Scheme depicting the cross section of the MscL pore, in its closed, expanded closed (leaning down in a bilayer with MT but gate still closed), open, and reclosed states. Approximate location of residues 12, 15, 20 and 41 are indicated. B) The pore area at different depths in the pore is approximated as the area of the pentamers formed by residues 12, 15, 20 and 41 of the homopentameric MscL. The areas for the same simulation set used in Fig. 1B are shown as well as the applied MT. The area defined by residues 41 is closest to the extracellular cavity; residues 12 and 15 represent the intracellular channel entrance (after the C-terminus); and residues 20 are close to the channel constriction.

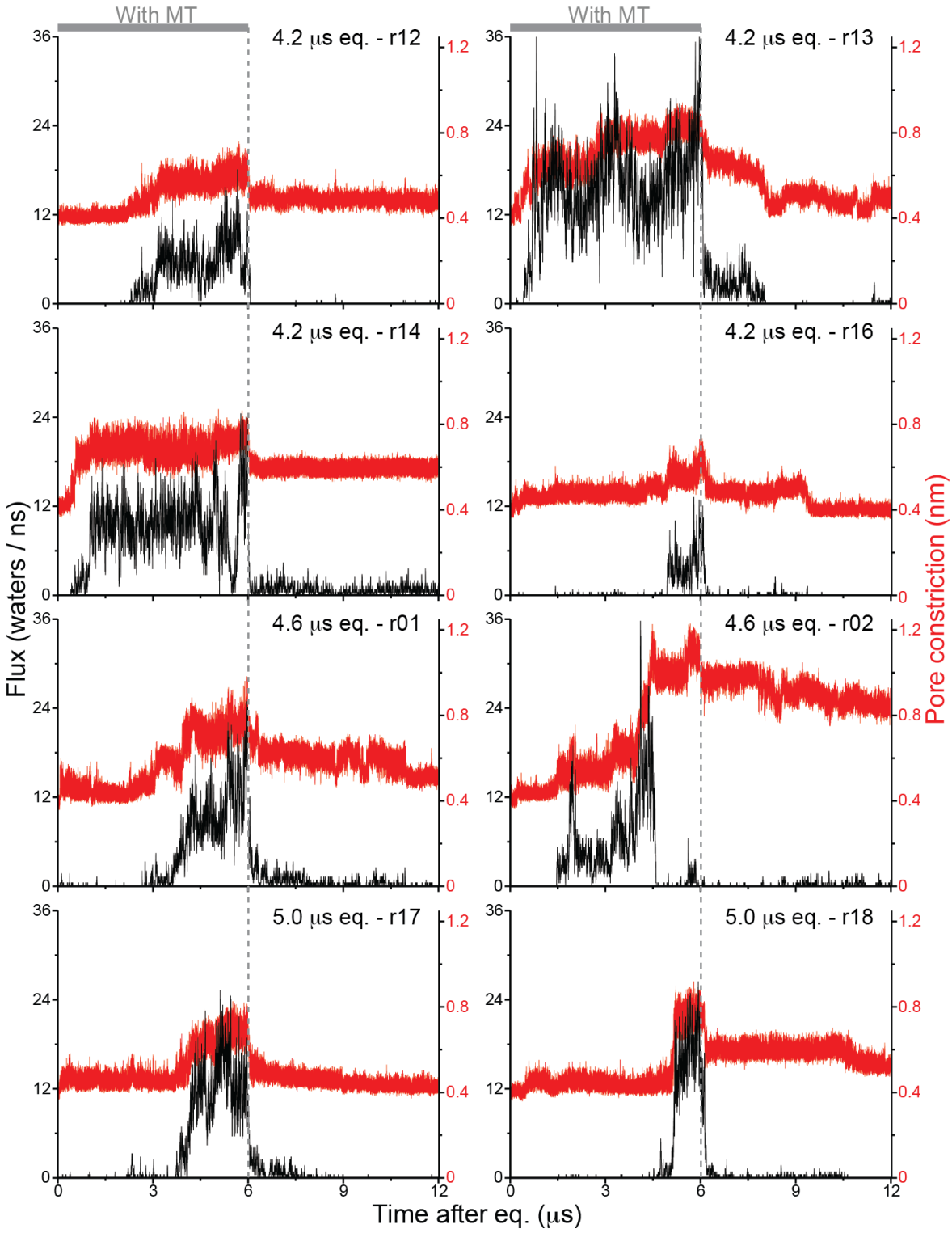
With MT
With MT
4.2 μs eq. - r12
4.2 μs eq. - r13
4.2 μs eq. - r14
4.2 μs eq. - r16
4.6 μs eq. - r01
4.6 μs eq. - r02
5.0 μs eq. - r17
5.0 μs eq. - r18
Flux (waters / ns)
Pore constriction (nm)
Time after eq. (μs)
0
12
24
36
0.4
0.8
1.2
3
6
9

Figure S2. MscL gating characteristics. To explore the overall channel gating characteristics of MscL, eight simulations where the channel had opened were selected, the MT removed, and each simulated further for 6 μs. Equilibrium time and repeat number is indicated for each simulation (see also Table S1). The water flux and the channel constriction radius are shown from the moment MT was applied. Note that in the 4.6 μs eq. – r02 simulation the water flux is blocked, even while under MT, without a tightening of the pore constriction. In this particular simulation the channel's C-terminus enters the pore, significantly blocking it and keeping the channel from reclosing. The significance of such an occurrence cannot be concluded from a single event, but the data is presented for completion (from Fig. 1C it can be seen that the average channel profile after reclosing remains close to the equilibrated crystal structure, despite the inclusion of this outlying case).

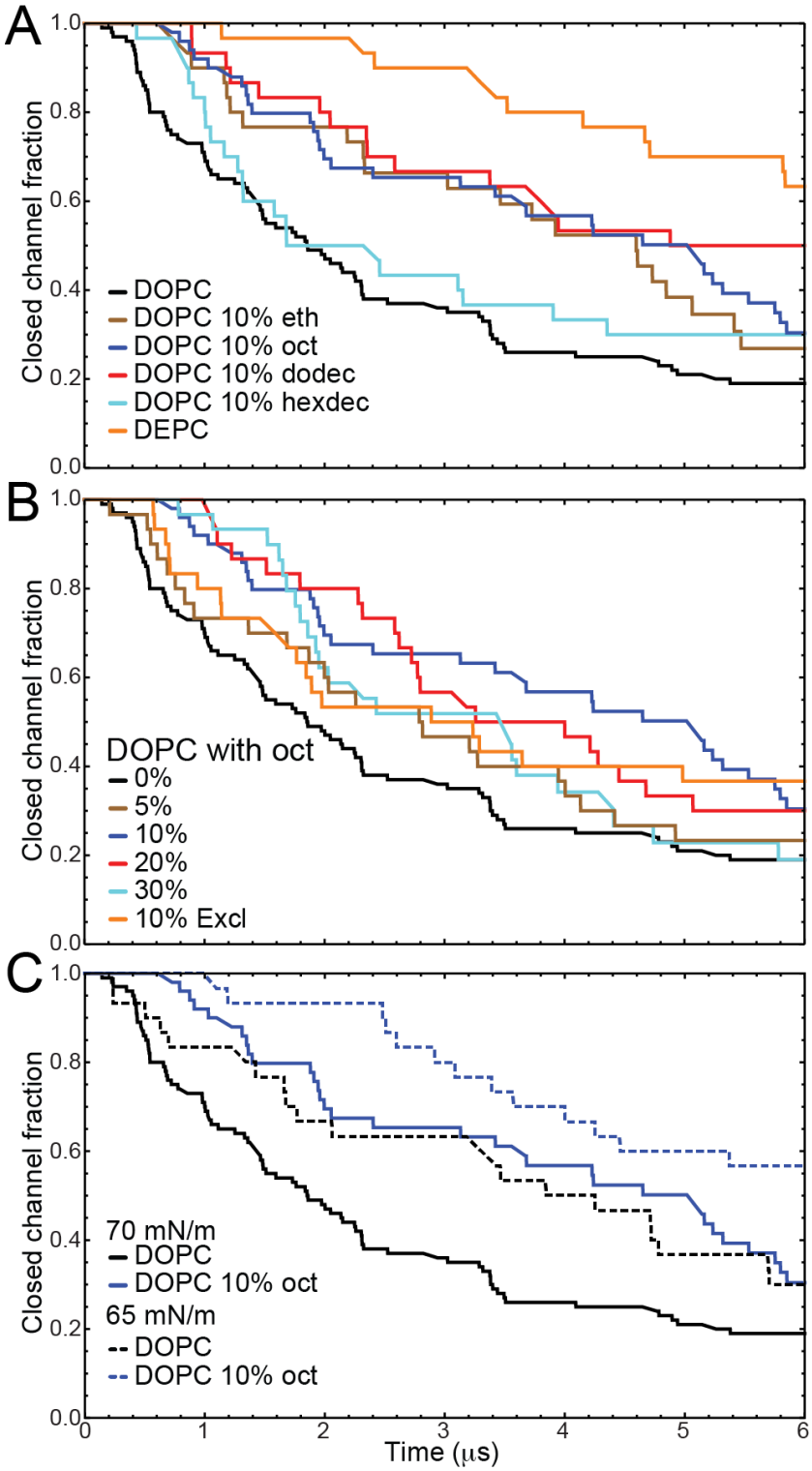

Figure S3. MscL channel survival graphs. For each bilayer environment/condition: different alcohols (A), octanol concentration (B), or 65 vs. 70 mN/m applied membrane tension (C), are compared by combining all the repeated simulation after applied membrane tension at that condition. The time to MscL channel opening is compared using Kaplan–Meier plots made with

the survival model fit in Wolfram Research, Inc., Mathematica, Version 9. All the simulations and channel opening times are listed in Table S1.

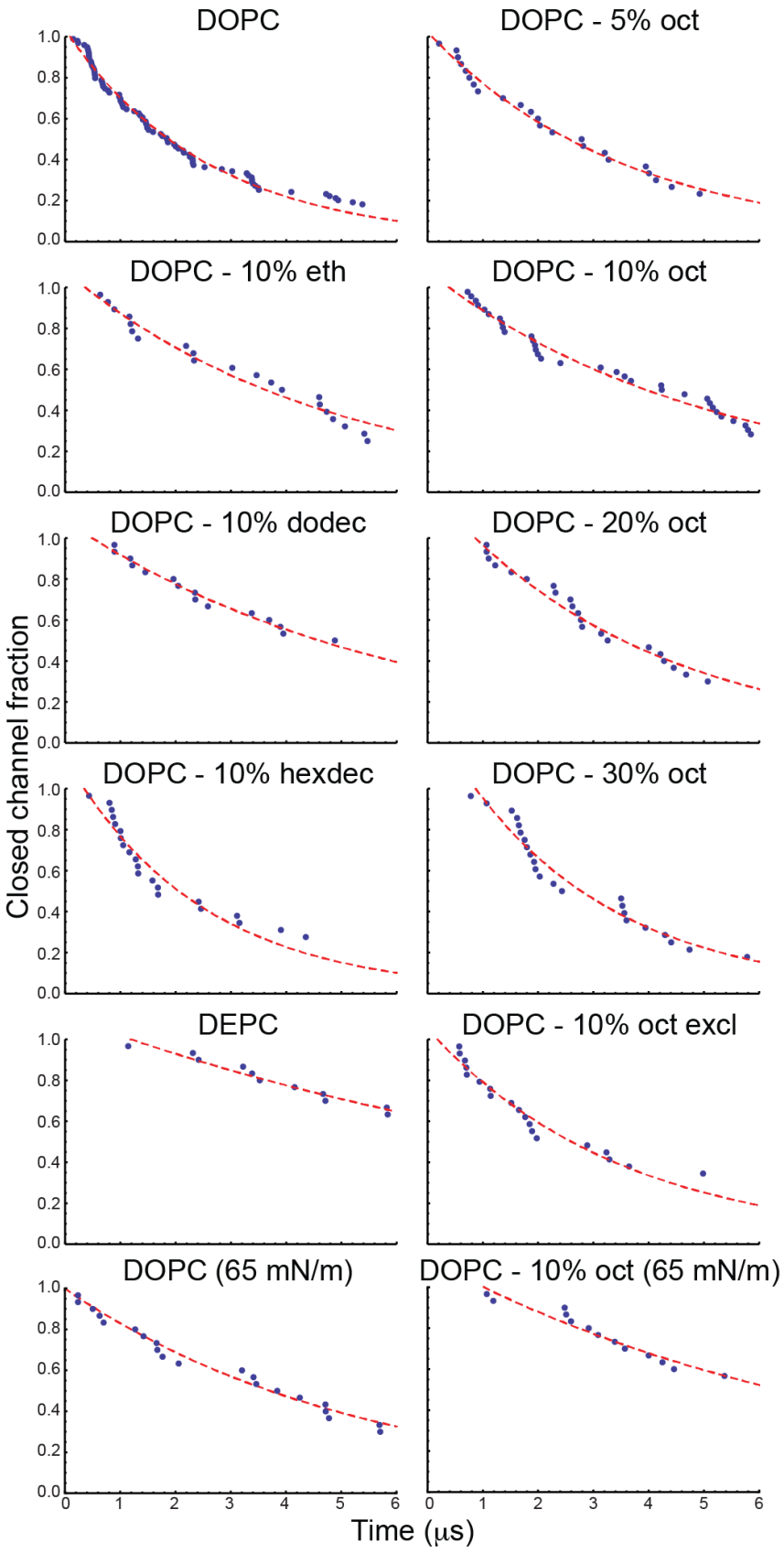
DOPC
DOPC - 5% oct
DOPC - 10% eth
DOPC - 10% oct
DOPC - 10% dodec
DOPC - 20% oct
DOPC - 10% hexdec
DOPC - 30% oct
DEPC
DOPC - 10% oct excl
DOPC (65 mN/m)
DOPC - 10% oct (65 mN/m)
Closed channel fraction
Time (μs)
0.0
0.2
0.4
0.6
0.8
1.0
0
1
2
3
4
5
6

Figure S4. MscL opening time fits. For each bilayer environment/condition the closed channel fraction was fit using a single exponential decay with a delay ($y = e^{-\lambda(x-d)}$) using the nonlinear model fit in Wolfram Research, Inc., Mathematica, Version 9. All the simulations and channel opening times are listed in Table S1 and the summary for each condition and fit output are listed in Table S2.

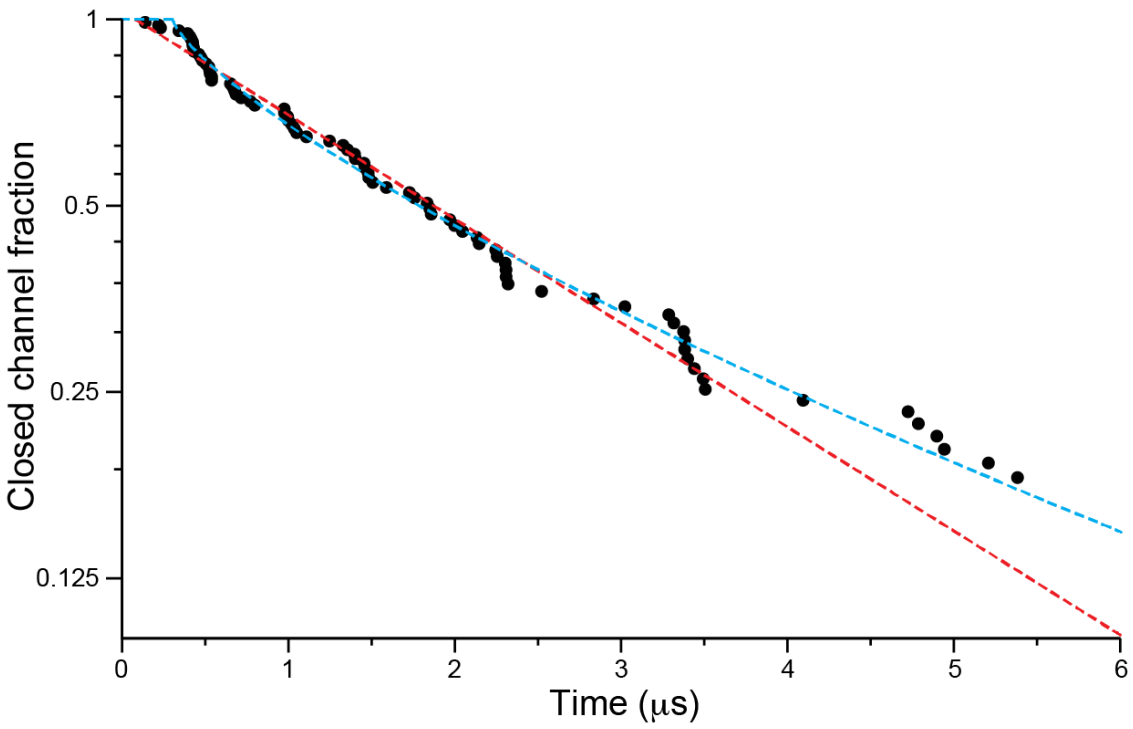

Figure S5. Detailed MscL opening kinetics. The closed channel fraction decay for DOPC (n = 100, black dots) are sown on a logarithmic scale with fits to a single exponential decay with a delay ($y = e^{-\lambda(x-d)}$, red dashed line) and a stretched exponential decay with a delay ($y = e^{-(\lambda(x-d))^{\beta}}$), blue dashed line). For the single exponential decay λ and d are 0.39 and 0.09, respectively, and for the stretched exponential decay λ, d and β are 2.85, 0.31 and 0.75, respectively, but the time when half the channels have opened ($t_{½}$) is very similar.

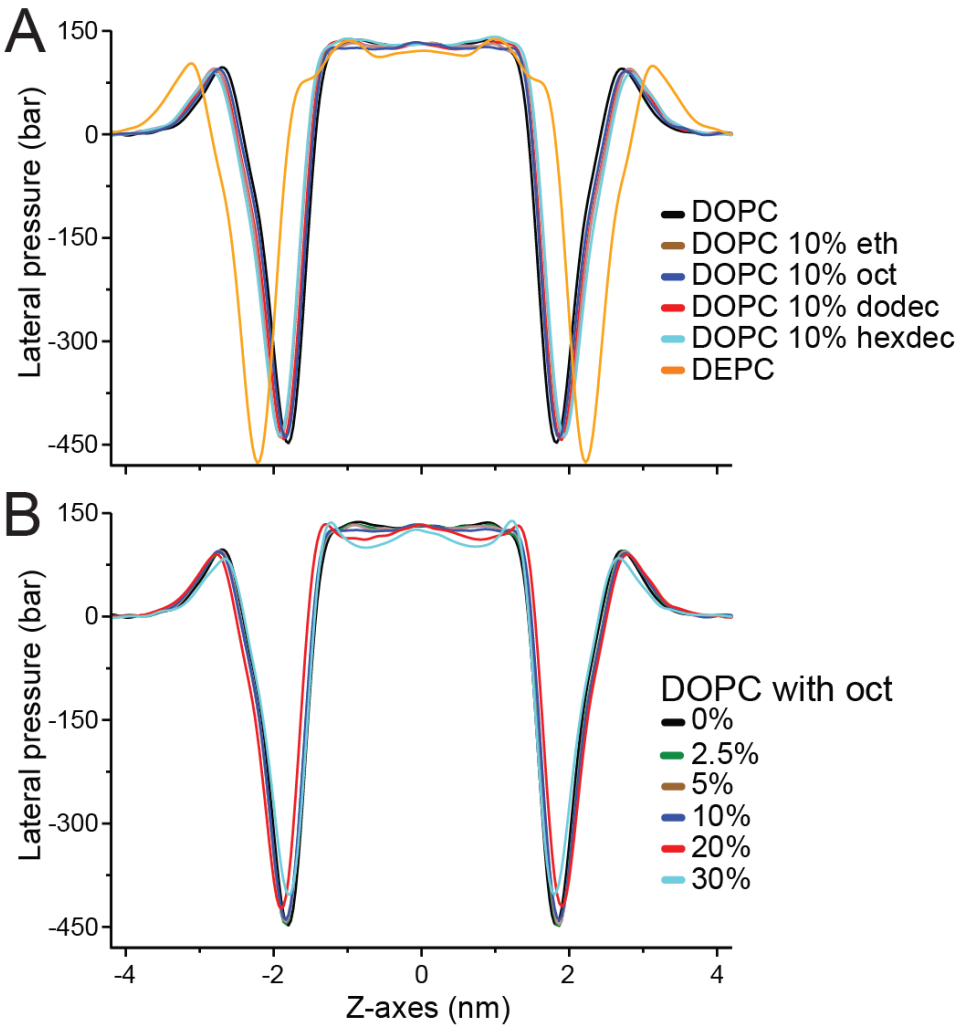

Figure S6. Lateral pressure profiles (LPPs). LPPs for each bilayer environment/condition: different alcohols (A) and different octanol concentrations (B).

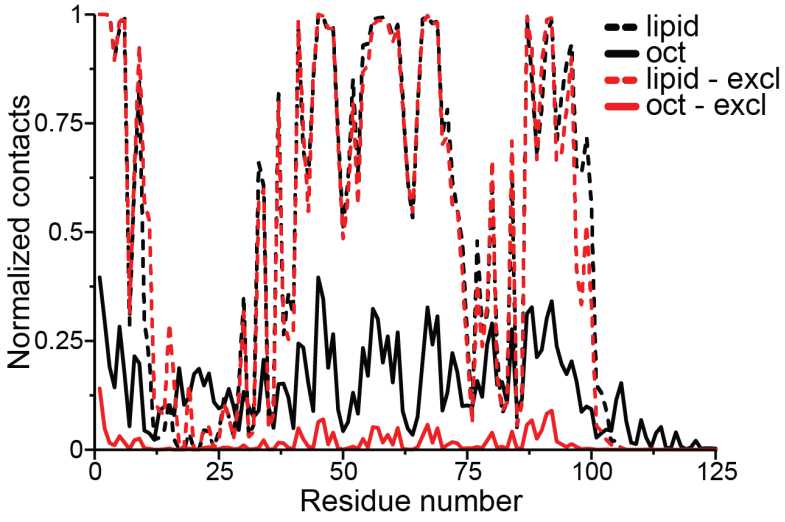

Figure S7. Octanol binding. To explore possible octanol (oct) preferred interactions/binding to MscL the normalized contacts (fraction of total simulation time spent in contact) between each MscL residue and octanol was calculated. For reference, the normalized contacts for the lipids linker region (GL1 and GL2 beads) were also calculated (lipid). Average results for all simulations with applied 70 mN/m MT and 10% oct (black) and with 10% oct Excl (red) are shown.

Table S1. Simulation summary[a]

This table is provided in the file "ja6b11091_si_002.xlsx" and can also be found at:

http://cgmartini.nl/images/applications/mscl/MscL_gating-TableS1.xlsx

[a]This simulation summary lists all the main simulations run for this study. For each simulation the bilayer environment/condition is listed as well as the applied membrane tension (MT), where 0* is no applied MT but regular 1 bar pressure coupling. The start time and length of each simulation is also listed as well as the time of MscL channel opening, measured by monitoring the water flux across the channel; see Supplementary Methods. In total these simulations sum up to over 2700 μs of simulation time, or over 10 ms after accounting for the ~4 times faster diffusion times at the Martini CG level.[2]

Table S2. MscL time to opening[a]

Condition	Repeat count	Bilayer broke	Channel opened	Fit adj. R^2	λ / μs^{-1}		d / μs		$t_{1/2}$ / μs		
					fit	se	fit	se	fit	se	95%[b]
DOPC	100	1	81	0.998	0.39	0.01	0.09	0.02	1.88	0.05	0.10
eth	30	2	21	0.996	0.21	0.01	0.36	0.10	3.62	0.26	0.56
5% oct	30	0	23	0.998	0.28	0.01	0.08	0.05	2.55	0.12	0.25
10% oct	50	4	33	0.997	0.19	0.01	0.38	0.07	3.95	0.19	0.39
20% oct	30	0	21	0.997	0.26	0.01	0.87	0.07	3.53	0.19	0.39
30% oct	30	2	23	0.992	0.36	0.02	0.87	0.08	2.78	0.20	0.41
dodec	30	0	15	0.999	0.17	0.01	0.49	0.08	4.60	0.25	0.54
hexdec	30	1	21	0.992	0.41	0.03	0.35	0.08	2.06	0.22	0.47
DEPC	30	0	11	0.999	0.09	0.01	1.19	0.18	8.85	0.73	1.67
10% oct Excl	30	1	19	0.998	0.29	0.02	0.18	0.09	2.60	0.24	0.51
DOPC-65[c]	30	0	21	0.998	0.19	0.01	0.00	0.08	3.71	0.22	0.46
10% oct-65[c]	30	0	13	0.999	0.13	0.01	1.01	0.17	6.34	0.60	1.35

[a]After applying membrane tension the time to channel opening was measured for repeated simulations with each bilayer environment; see Supplementary Methods. Details for each simulation are reported in Table S1. For each bilayer environment the open channel fraction was fit using a single exponential decay with a delay ($y = e^{-\lambda(x-d)}$); see Fig. S3 for all fits. Here we report for each bilayer environment/condition: the number of repeats, the number of simulations where the bilayer broke before the channel opened, the number of repeats where the channel opened before simulation was stopped (6 μs), the adjusted R^2 of the fits, the best fit parameter and parameter standard error (se) for λ and d, and the time when half the channels have opened ($y = 0.5$) with propagated se.

[b]Errors for the time of half the channel population to be opened ($t_{1/2}$) were estimated by propagating the max/min of the 95% confidence intervals for the fitted parameters λ and d.

[c]With applied MT of 65 mN/m instead of the regular 70 mN/m. Note, the 5 mN/m reduction in applied MT has similar effect on $t_{1/2}$ as the 10 mol% added short-chain alcohols—see also Fig. S3C—indicating that the alcohols effect on MscL gating threshold is on the order of 5 mN/m.

Table S3. Changes in bilayer properties[a]

Condition	Area per lipid / nm^2		Area compressibility / mN/m			Average tail order parameter		Lipid diffusion / 10^{-5} cm^2/s		Bilayer thickness / nm	
	mean	sd	mean	sd	se	mean	sd	mean	se	mean	sd
No-tension											
DOPC	0.669	0.004	402	16	6	0.328	0.007	0.038	0.001	4.451	0.022
eth	0.673	0.005	397	12	5	0.326	0.007	0.042	0.005	4.441	0.023
2.5% oct	0.672	0.005	428	17	7	0.329	0.007	0.040	0.001	4.448	0.023
5% oct	0.675	0.005	411	18	8	0.329	0.007	0.039	0.003	4.442	0.023
10% oct	0.681	0.005	400	18	8	0.329	0.007	0.037	0.003	4.434	0.023
20% oct	0.693	0.005	395	9	4	0.329	0.007	0.039	0.001	4.412	0.023
30% oct	0.708	0.005	390	20	9	0.326	0.007	0.044	0.001	4.384	0.023
dodec	0.685	0.005	400	9	4	0.334	0.007	0.041	0.004	4.440	0.023
hexdec	0.692	0.005	405	11	5	0.334	0.007	0.041	0.002	4.443	0.023
DEPC	0.664	0.005	429	19	8	0.340	0.008	0.025	0.003	5.118	0.028
With 65 mN/m membrane tension											
DOPC	1.069	0.016	49	3	1	0.136	0.006	0.074	0.003	3.250	0.037
eth	1.101	0.017	48	4	2	0.134	0.006	0.067	0.001	3.200	0.038
2.5% oct	1.084	0.017	48	3	1	0.136	0.007	0.069	0.001	3.228	0.039
5% oct	1.094	0.017	51	3	1	0.136	0.007	0.072	0.000	3.217	0.038
10% oct	1.109	0.017	51	4	2	0.137	0.007	0.073	0.004	3.203	0.037
20% oct	1.139	0.017	50	3	1	0.137	0.007	0.081	0.012	3.170	0.037
30% oct	1.175	0.018	51	2	1	0.138	0.007	0.088	0.001	3.137	0.036
dodec	1.112	0.017	50	3	1	0.138	0.007	0.080	0.003	3.213	0.038
hexdec	1.117	0.018	48	3	1	0.138	0.007	0.072	0.012	3.227	0.039
DEPC	1.061	0.018	49	4	2	0.136	0.007	0.043	0.003	3.669	0.049

[a]Bilayer properties were calculated for all considered bilayer environments both with and without applies tension (65 mN/m); for details see Supplementary Methods. Standard errors (se) for the area per lipid, average tail order parameter, and bilayer thickness were omitted, as all values are <0.001.

Supporting Information References:

(1) Berendsen, H. J. C.; Postma, J. P. M. *J. Chem. Phys.* **1984**, *81*, 3684.
(2) Marrink, S. J.; Risselada, H. J.; Yefimov, S.; Tieleman, D. P.; De Vries, A. H. *J. Phys. Chem. B* **2007**, *111*, 7812.
(3) Monticelli, L.; Kandasamy, S. K.; Periole, X.; Larson, R. G.; Tieleman, D. P.; Marrink, S. J. *J. Chem. Theory Comput.* **2008**, *4*, 819.
(4) Chang, G.; Spencer, R. H.; Lee, A. T.; Barclay, M. T.; Rees, D. C. *Science* **1998**, *282*, 2220.
(5) Steinbacher, S.; Bass, R.; Strop, P.; Rees, D. C. In *Mechanosensitive Ion Channels, Part A*; Current Topics in Membranes; Elsevier, 2007; Vol. 58, pp 1–24.
(6) Kabsch, W.; Sander, C. *Biopolymers* **1983**, *22*, 2577.
(7) Hess, B.; Kutzner, C.; van der Spoel, D.; Lindahl, E. *J. Chem. Theory Comput.* **2008**, *4*, 435.
(8) Lindahl, E.; Edholm, O. *J. Chem. Phys.* **2000**, *113*, 3882.
(9) Ollila, O. H. S.; Risselada, H. J.; Louhivuori, M.; Lindahl, E.; Vattulainen, I.; Marrink, S. J. *Phys. Rev. Lett.* **2009**, *102*, 078101.